Neuropeptide release by efficient recruitment of diffusing cytoplasmic secretory vesicles

Weiping Han*†, Yuen-Keng Ng*, Daniel Axelrod‡, and Edwin S. Levitan*§

*Department of Pharmacology, University of Pittsburgh, Pittsburgh, PA 15261; and ‡Biophysics Research Division, University of Michigan, Ann Arbor, MI 48109

Edited by Charles F. Stevens, The Salk Institute for Biological Studies, La Jolla, CA, and approved October 11, 1999 (received for review July 28, 1999)

Neuropeptides are slowly released from a limited pool of secretory vesicles. Despite decades of research, the composition of this pool has remained unknown. Endocrine cell studies support the hypothesis that a population of docked vesicles supports the first minutes of hormone release. However, it has been proposed that mobile cytoplasmic vesicles dominate the releasable neuropeptide pool. Here, to determine the cellular basis of the releasable pool, single green fluorescent protein-labeled secretory vesicles were visualized in neuronal growth cones with the use of an inducible construct or total internal reflection fluorescence microscopy. We report that vesicle movement follows the diffusion equation. Furthermore, rapidly moving secretory vesicles are used more efficiently than stationary vesicles near the plasma membrane to support stimulated release. Thus, randomly moving cytoplasmic vesicles participate in the first minutes of neuropeptide release. Importantly, the preferential recruitment of diffusing cytoplasmic secretory vesicles contributes to the characteristic slow kinetics and limited extent of sustained neuropeptide release.

Neuropeptides participate in the perceptions of pain, pleasure, and appetite and regulate peripheral organs (1). More than 30 years ago it was determined that even the most intense stimuli (e.g., sustained depolarization with Ca^{2+} or Ba^{2+}) induce slow release of only a fraction of stored neuropeptides, suggesting the presence of a special, releasable pool of secretory vesicles (2, 3). The presence of such a limited pool ensures that the contents of nerve terminals are not exhausted with a single bout of action potentials. This is particularly important for neuropeptides because they are synthesized in cell bodies and then transported over long distances to sites of release (1). Microscopy studies with nerve terminals and growth cones have failed to reveal a spatially defined, releasable pool (2, 4). However, the finding that the releasable neuropeptide pool is similar in size to the mobile pool of vesicles in the cytoplasm led to the proposal that release is limited by vesicle mobility instead of localization (4). Yet, depletion of mobile peptidergic vesicles by exocytosis has not been observed. Furthermore, recent experiments with endocrine chromaffin cells have verified the common assumption that the first minutes of release are supported exclusively by vesicles docked to the plasma membrane (5–7). Thus, a parsimonious interpretation of published findings so far is that the apparent global loss of neuropeptide-containing vesicles that accompanies depolarization reflects a redistribution of unprimed cytoplasmic vesicles and that only docked vesicles support neuropeptide secretion.

The inability of past studies to directly prove that the releasable neuropeptide pool is composed solely of docked vesicles indicates that high-resolution measurements of vesicle behavior in growth cones would be informative. However, because secretory vesicles are so abundant in growth cones, previous imaging studies could not follow the movement of individual vesicles at this site of robust neuropeptide release. Hence, it is not known how vesicles move within growth cones or whether mobile vesicles participate in secretion responses. To overcome this limitation, methods for monitoring the behavior of single secretory vesicles are needed.

One approach that has proven useful for imaging secretory vesicles in endocrine chromaffin cells is to use microscopy techniques that feature illumination limited to a region near the plasma membrane. This has been accomplished with oblique epiillumination or with total internal reflection fluorescence microscopy (TIRFM, also called evanescent-field microscopy) (6–9). With the latter technique, only the region of a cultured cell very close to the substrate (e.g., a glass coverslip) is illuminated by an exponentially decaying evanescent field (10). Therefore, because only vesicles close to the plasma membrane are visible, it is possible to follow docking and release with TIRFM. Studies with bovine chromaffin cells have shown that docked acridine orange-labeled secretory vesicles are abundant and wander very slowly as if they are diffusing within a drifting cage. On the other hand, some cytoplasmic vesicles quickly move to and from the membrane in a nonrandom, unidirectional manner. Importantly, such vesicles are rare and, thus, do not appear to contribute significantly to the first minutes of release. Whether similar secretory vesicle motion is seen at sites of neuropeptide release is not known because TIRFM has not been applied to the study of growth cones.

Another potential strategy for imaging single secretory vesicles in growth cones could be to label fewer vesicles at sites of release. It is not clear how limited or specific labeling could be accomplished with acridine orange. However, we reasoned that because green fluorescent protein (GFP) labeling depends on gene expression, this could be accomplished with an inducible construct. The ecdysone-inducible expression system is a well established, tightly regulated system for heterologous expression in mammalian cells (11). To our knowledge, application of such an inducible system to the study of regulated secretion has not been attempted previously.

Here, we describe how the use of TIRFM and a new, bright inducible GFP-tagged neuropeptide enable imaging of single secretory vesicles in live growth cones. With these techniques, we address how secretory vesicles move at avid sites of neuropeptide release and directly test whether neuropeptide secretion is supported by a stable population of docked vesicles. Our results demonstrate that vesicle motion and the releasable pool are different in growth cones than predicted from conventional models derived from endocrine cells.

Materials and Methods

Constructs. Initially, proANF-EGFP (4) was subcloned into an ecdysone-inducible expression vector (Invitrogen). However, fluorescent vesicles produced after transfection into PC12 cells

Abbreviations: TIRFM, total internal reflection fluorescence microscopy; GFP, green fluorescent protein.

†Present address: Center for Basic Neuroscience, University of Texas Southwestern Medical Center, Dallas, TX 75235.

§To whom reprint requests should be addressed at: E1351 Biomedical Science Tower, Department of Pharmacology, University of Pittsburgh, Pittsburgh, PA 15261. E-mail: Levitan@server.pharm.pitt.edu.

The publication costs of this article were defrayed in part by page charge payment. This article must therefore be hereby marked "*advertisement*" in accordance with 18 U.S.C. §1734 solely to indicate this fact.

with Tfx-50 (Promega) and induction with 1 μM muristerone A for 2–4 hr were dim. Therefore, the EGFP variant was excised from the original construct by digestion with *Age*I and *Not*I and replaced with a PCR product of Emerald GFP (ref. 12; Emd; Packard) to generate a proANF-Emd vector. Vesicles labeled by this new construct were ≈3-fold more fluorescent than those with proANF-EGFP. The ecdysone-inducible version was generated by ligating the proANF-Emd fusion cDNA into the pIND vector (Invitrogen) at the *Not*I and *Eco*RI sites. In some TIRFM experiments, a stable line of proANF-Emd-expressing PC12 cells was used. This line was generated by cotransfection of the constitutively active proANF-Emd plasmid with a neomycin resistance gene-containing plasmid followed by antibiotic selection.

Experimental Procedures. PC12 cells were plated on polylysine-coated glass coverslips and treated with 50 ng/ml 2.5 S nerve growth factor (Life Technologies, Gaithersburg, MD) for 2 days before imaging experiments. Only one growth cone was analyzed from each cell. Fluorescent vesicles labeled with the ecdysone-inducible system were viewed on an inverted Nikon Diaphot epifluorescence microscope equipped with either a ×100 1.3-numerical aperture (NA) oil-immersion objective (Olympus) or a ×60 1.4-NA oil-immersion objective (Olympus), a 75-W xenon lamp in an Optiquip Universal Lamphouse for illumination, and a Photometrics Quantix cooled charge-coupled device camera for image acquisition. TIRFM experiments, which utilized the conventional proANF-Emd construct, were performed on an upright Olympus microscope equipped with an Olympus ×60 0.9-NA water-immersion objective, a trapezoidal prism fabricated out of a truncated equilateral triangular prism with a refractive index of 1.648 (Rolyn Optics, Covina, CA), a single lens (Edmund Scientific, Barrington, NJ) for focusing the laser beam, and a 488-nm Spectraphysics argon laser as described by Axelrod (10). To ensure optical contact, a drop of low-fluorescence immersion oil was placed on top of the prism before it was raised on the condenser mount to come in contact with the coverslip upon which cells were grown. The facts that the refractive index of the glass is so much higher than that of cells and that the incident angle of the laser beam is 60° ensures that illumination will be via an evanescent field and not by oblique epiillumination. In fact, total internal reflection of the laser beam was visible. Although the characteristic penetration depth cannot be measured in live growth cones, we estimate a value of 110 nm for our setup, assuming a refractive index for the growth cone of 1.38. The exponential drop-off in this evanescent field ensures that fluorescence originating from 330 nm above the coverslip will be only 5% as strong as signals originating from right next to the coverslip and 13.5% of signals from 110 nm above the coverslip. A conventional epifluorescence xenon lamp was also present on the microscope so that epifluorescence and TIRFM images could be compared by controlling shutters (Uniblitz) for the xenon lamp or the laser. All data acquisition and analysis were performed with INOVISION software running on a workstation (O2; Silicon Graphics, Mountain View, CA). As a control, trajectory data were acquired from paraformaldehyde-fixed cells. Apparent vesicle movement, which could have been caused by stage drift or misinterpretation of noise by the tracking software, was not significant (i.e., calculated diffusion coefficients for fixed vesicles were $<10^{-13}$ cm^2/s). Control of hardware and image processing utilized INOVISION software running on a Silicon Graphics O2 computer.

Normal bathing solution contained 140 mM NaCl, 5.4 mM KCl, 5 mM $CaCl_2$, 0.8 mM $MgCl_2$, 10 mM glucose, and 10 mM Na-Hepes, pH 7.4. Depolarization-evoked peptide release was induced by superfusing with 100 mM KCl, 45 mM NaCl, 5 mM $BaCl_2$, 0.8 mM $MgCl_2$, 10 mM glucose, and 10 mM Na-Hepes, pH 7.4. Ba^{2+} has been used since the earliest measurements of the releasable neuropeptide pool (3). Furthermore, Ba^{2+} and Ca^{2+} act by a similar mechanism to evoke peptide release (13). Also, we have found that secretion responses to Ba^{2+} and Ca^{2+} are very similar (X. Lu and E.S.L., data not shown). Indeed, either Ca^{2+} or Ba^{2+} can deplete mobile vesicles. However, Ba^{2+}, unlike Ca^{2+}, does not evoke growth cone movement under our conditions. For this reason, depolarization in the presence of Ba^{2+} was used in all of the presented studies. All imaging experiments were performed at 25°C.

Image Processing for Fig. 4. Our goal was to generate a method for quantitating changes in either rapidly diffusing "mobile" vesicles or stationary vesicles. The basic approach was to acquire pairs of images 1 s apart. Then, a pixel-by-pixel "subtraction function" (which produces an image made up of pixels that became brighter) followed by "feature extraction" (which rejects pixels that are not part of a vesicle-sized object) was used to generate an image that shows only vesicles that took large steps. Similarly, using a bit-wise "and" function (which only displays pixels that remained bright) and "feature extraction" produces an image of stationary vesicles. Integrating the signals after these "subtraction" and "and" operations then yields values that are dominated by the numbers of rapidly moving and stationary vesicles, respectively. To reduce the variability of these measurements, five images were collected at 1 Hz every minute. This provided multiple pairs (e.g., image1 and image2, image2 and image3, etc.) for calculation of an average value for the mobile and stationary pools each minute. Results then were combined from independent experiments to yield the data in Fig. 4*B*.

Results

Two methods were used for imaging single neuropeptide-containing secretory vesicles in growth cones. First, Emerald GFP-tagged proANF (atrial natriuretic factor; ref. 14) was cloned into an inducible mammalian expression vector (see *Materials and Methods*). After transfection and nerve growth factor treatment, expression of the GFP fusion protein was activated for 2–4 hr. Epifluorescence microscopy then revealed growth cones with a limited number of GFP-labeled vesicles (Fig. 1*A*). A second approach utilized TIRFM to view growth cones with an abundance of labeled vesicles (Fig. 1*B Upper*). With TIRFM, only a very thin optical section near the plasma membrane in contact with a coverslip is illuminated (10) so that detection of single GFP-labeled vesicles in growth cones is possible (Fig. 1*B Lower*). Thus, the use of an inducible construct or TIRFM enabled time-lapse imaging of the movements of single secretory vesicles.

Particle tracking then was used to determine the trajectories of single vesicles within growth cones. In addition to standard two-dimensional movements in the plane of focus (i.e., the *xy* plane), movement perpendicular to the coverslip was measured with TIRFM. This is possible because the intensity of evanescent wave illumination produced by total internal reflection drops off exponentially in the *z* axis with a characteristic penetration depth that is a fraction of a wavelength of the incident light (10). Two important features were displayed in secretory vesicle trajectories deduced from either epifluorescence measurements of vesicles labeled with the inducible construct (Fig. 2*A*) or TIRFM experiments (Fig. 2*B*). First, a wide range of speeds of movement was detected in the *xy* plane (Fig. 2 *A* and *B Left*). This agrees with previous measurements of single secretory vesicles in nerve growth factor-treated PC12 cell bodies and the results of FRAP (fluorescence recovery after photobleaching) experiments on growth cones (4). Second, movement in general appears to be random. For example, examination of 20 vesicles did not reveal unidirectional movement to and from the plasma membrane in growth cones (Fig. 2*B Right*). Therefore, we turned our attention to analyzing secretory vesicle trajectories within growth cones.

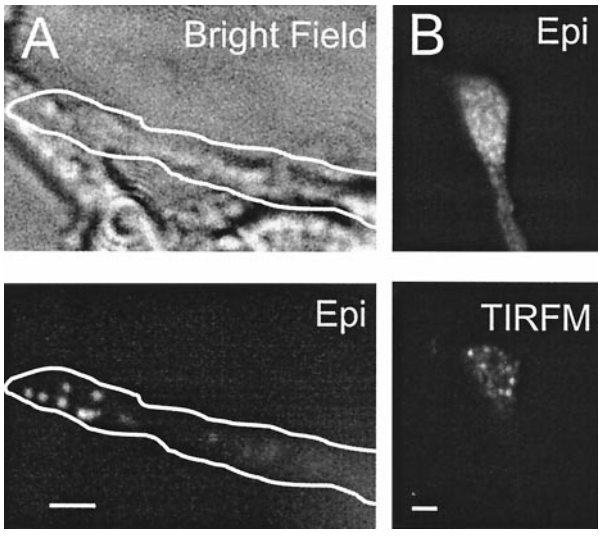

Fig. 1. Single GFP-labeled secretory vesicles in neuronal growth cones. (*A*) Cells were treated with 1 μM muristerone to activate the inducible expression construct before imaging. (*Upper*) Bright-field view of neurites illuminated with a Hoffman condenser. (*Lower*) Epifluorescence image shows that single secretory vesicles labeled with proANF-Emd are evident in one growth cone. Outline shows transfected neurite. (*B Upper*) Conventional epifluorescence image of a growth cone expressing the constitutive proANF-Emd construct. Note that it is difficult to resolve individual vesicles. (*Lower*) Single secretory vesicles are evident in the TIRFM image of the same growth cone. (Bar = 2 μm.)

Two criteria were used to test whether vesicle movement conforms to the diffusion equation. First, we examined whether the square of the two-dimensional distance covered (d^2) by vesicles increases linearly with time as is predicted by the equation: $d^2 = 4Dt$, where t is time and D is the diffusion coefficient (15). As can be seen in Fig. 3*A*, the trajectories of slow "immobile" and fast "mobile" vesicles satisfy this criterion. Second, we examined whether the variation in the value of d for a fixed time period ($t_c = 1.1$ s) is fit by diffusion theory (16). This involved fitting a cumulative plot of the percentage of trajectory steps ($100 \times N/N_{total}$) vs. two-dimensional distance (d) to the equation: $100 \times N/N_{total} = 1 - \exp(-d^2/4Dt_c)$. As can be seen in Fig. 3*B*, data from both slow and fast vesicles are well fit by this equation. Therefore, vesicles appear to walk randomly within growth cones, albeit at very different rates.

The data in Fig. 3*B* also indicate that a limited data set can be used to identify rapidly moving vesicles. For example, if a vesicle takes a large step (e.g., 150 nm) within a second, it is virtually certain that it is a mobile vesicle. Similarly, a vesicle that is nearly stationary for this period of time could be a mobile vesicle that happened to slow down as part of its random movement. However, it is more likely that it is an immobile vesicle. With this knowledge in hand, we developed an image-processing protocol to preferentially display either rapidly diffusing or stationary vesicles (see *Materials and Methods*).

This assessment method was applied to data acquired from experiments in which depolarization-evoked peptide release was monitored with TIRFM. Importantly, depletion of peptide from near the plasma membrane detected by TIRFM was greater at all time points measured (i.e., every minute) than total release from the same growth cones measured by epifluorescence. For example, after 6 min of stimulation, peptide released in the region viewed by TIRFM was 1.55 ± 0.11 times more than the $34 \pm 5\%$ peptide lost from the whole growth cone ($P < 0.01$, $n = 5$). Therefore, release must occur from the very thin region that is viewed by TIRFM (see *Materials and Methods*) into the spaces known to exist between the polylysine substrate and the growth cone (17). Because the released peptide is then free to rapidly diffuse away into the bulk medium, release from the bottom of the growth cone is detectable as a loss of GFP fluorescence.

Conventional models posit that mobile cytoplasmic vesicles must pass through a long-lived docked state before undergoing release. Indeed, in bovine chromaffin cells such docked vesicles account for the first 2 min of release. This predicts that stimulation of secretion should deplete stationary vesicles near the plasma membrane faster and more efficiently than rapidly moving vesicles. However, as can be seen in the processed images shown in Fig. 4*A*, release is accompanied by a marked depletion of rapidly moving vesicles. In contrast, a smaller fraction of peptide is lost from stationary vesicles near the plasma membrane. In fact, some stationary vesicles remained visible throughout whole experiments. Presumably, such vesicles are members of the reserve pool. The preferential depletion of mobile vesicles was evident in all five growth cones examined (Fig. 4*B*). Furthermore, depletion kinetics for stationary vesicles was comparable, or possibly slower, than depletion of mobile vesicles. Thus, loss of stationary vesicles may represent release from mobile

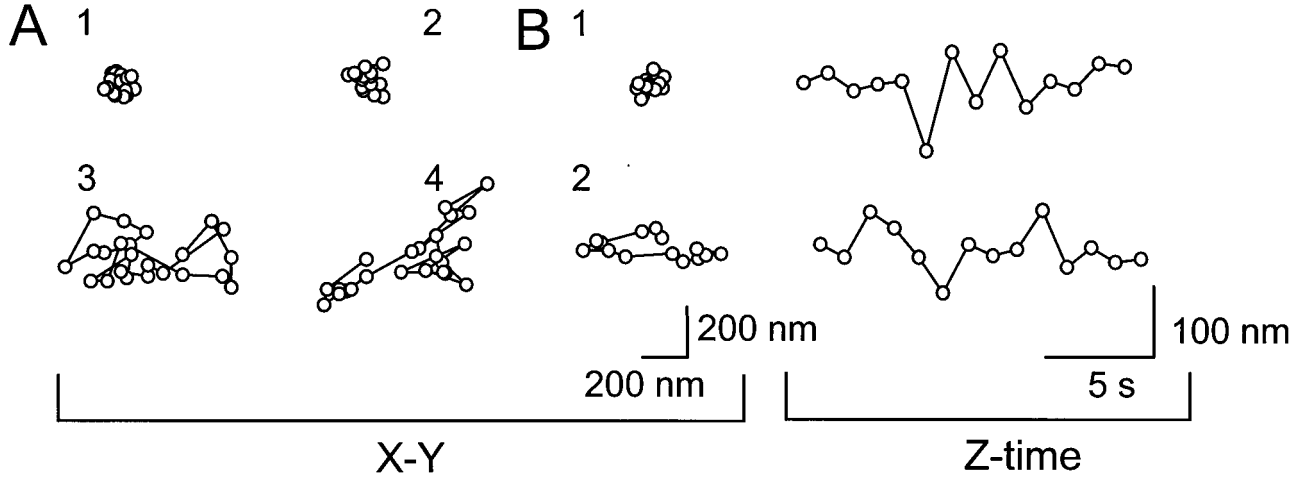

Fig. 2. Secretory vesicle trajectories within growth cones. (*A*) Examples from vesicles labeled with the inducible construct. (*B*) Examples detected by TIRFM. The *xy* trajectory and the simultaneous movement over time perpendicular to the substrate are shown for two vesicles. Images were acquired at 1 Hz. Note that motion in all dimensions appears to be random. Furthermore, a great range of vesicle speeds is evident.

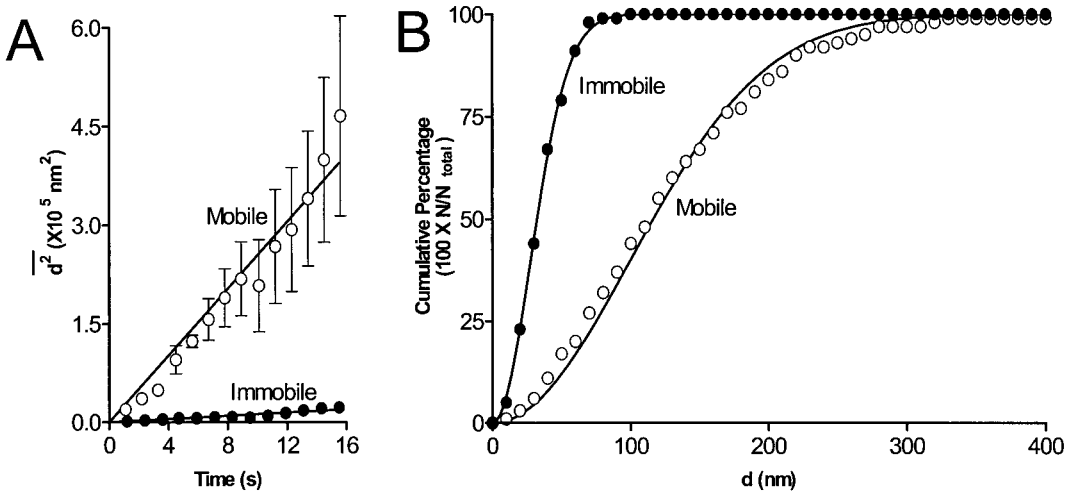

Fig. 3. Secretory vesicles move by diffusion. (*A*) d^2 vs. time plots for rapid, mobile, and slow, immobile vesicles. Note that both sets of data can be fit with straight lines yielding diffusion coefficients of 6.1×10^{-11} cm^2/s for the mobile vesicles and 3.1×10^{-12} cm^2/s for the immobile vesicles. $n \geq 15$ for each point. (*B*) Cumulative plots of number of trajectory steps vs. distance traveled. Note that both sets of data can be fit by the relationship predicted by diffusion (see text). Data included 152 points from 6 representative immobile vesicles and 145 points from 7 representative mobile vesicles labeled with the inducible construct sampled at 0.9 Hz. Calculated diffusion coefficients were 4.6×10^{-11} cm^2/s for the mobile vesicles and 3.3×10^{-12} cm^2/s for the immobile vesicles.

vesicles that randomly paused rather than from docked vesicles. At the very least, these results show that mobile vesicles are depleted more efficiently than immobile vesicles very near the plasma membrane.

The depletion of rapidly diffusing vesicles could represent immobilization (e.g., by replacing docked with unprimed vesicles), exocytosis, or redistribution away from the plasma membrane. The latter option has been excluded by previous confocal microscopy experiments (4). To directly discriminate between the other possibilities, we studied growth cones in which all or nearly all vesicles labeled with the inducible construct were mobile. This selection from the majority with both mobile and immobile vesicles was necessary so that interconversion could not significantly affect our analysis. Epifluorescence microscopy was used to image an optical section far thicker than TIRFM. Furthermore, total neuropeptide content was assayed by measuring the integrated epifluorescence signal (18). Our goal was to examine the impact of stimulation on release from rapidly moving vesicles. If the efficient depletion of these vesicles is caused by immobilization, then a conversion of rapidly moving vesicles to stationary vesicles should be evident in time lapse experiments. Also, no decrease in the integrated epifluorescence signal should be seen in growth cones containing exclusively rapidly moving vesicles. On the other hand, if mobile vesicles undergo exocytosis, time lapse imaging should show a disappearance of mobile vesicles accompanied by a decrease in the total epifluorescence signal.

Fig. 5*A* shows that stimulation caused a decrease in the total neuropeptide content in four growth cones that expressed nearly all rapidly moving vesicles. Indeed, in one case, all vesicles

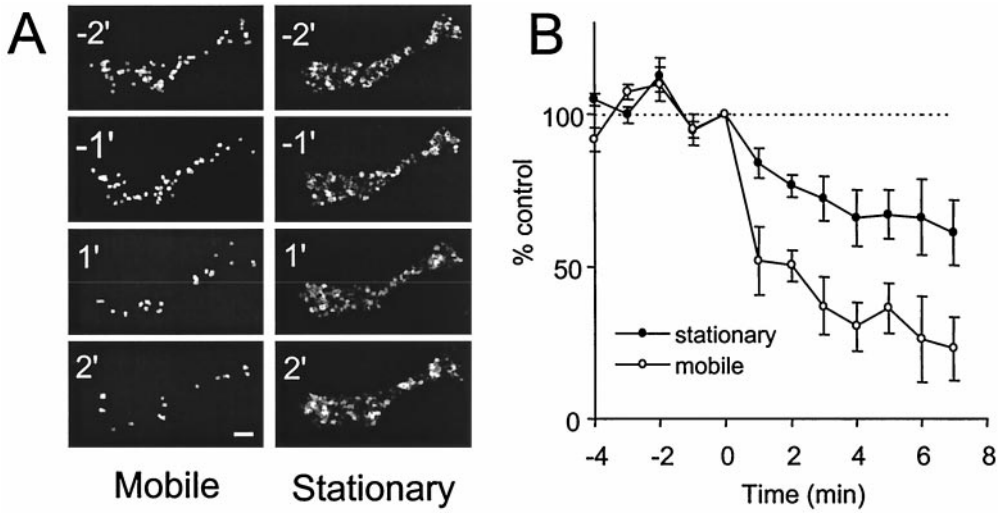

Fig. 4. Secretion depletes mobile secretory vesicles viewed by TIRFM in growth cones. (*A*) Image processing was used to display vesicles that took large steps (''mobile'') or that were stationary. Note that after depolarization, mobile vesicles are depleted whereas stationary vesicles show little change. (Bar = 2 μm.) (*B*) Quantitation from five experiments. Sustained depolarization started at 0 min. Mobile vesicle depletion was greater than stationary vesicle depletion. Furthermore, mobile vesicle depletion was at least as rapid as for stationary vesicles. Finally, although the measurement of mobile vesicles is not prone to contamination by slow, ''immobile'' vesicles, mobile vesicles occasionally stop and, hence, contribute to the measurement of stationary vesicles.

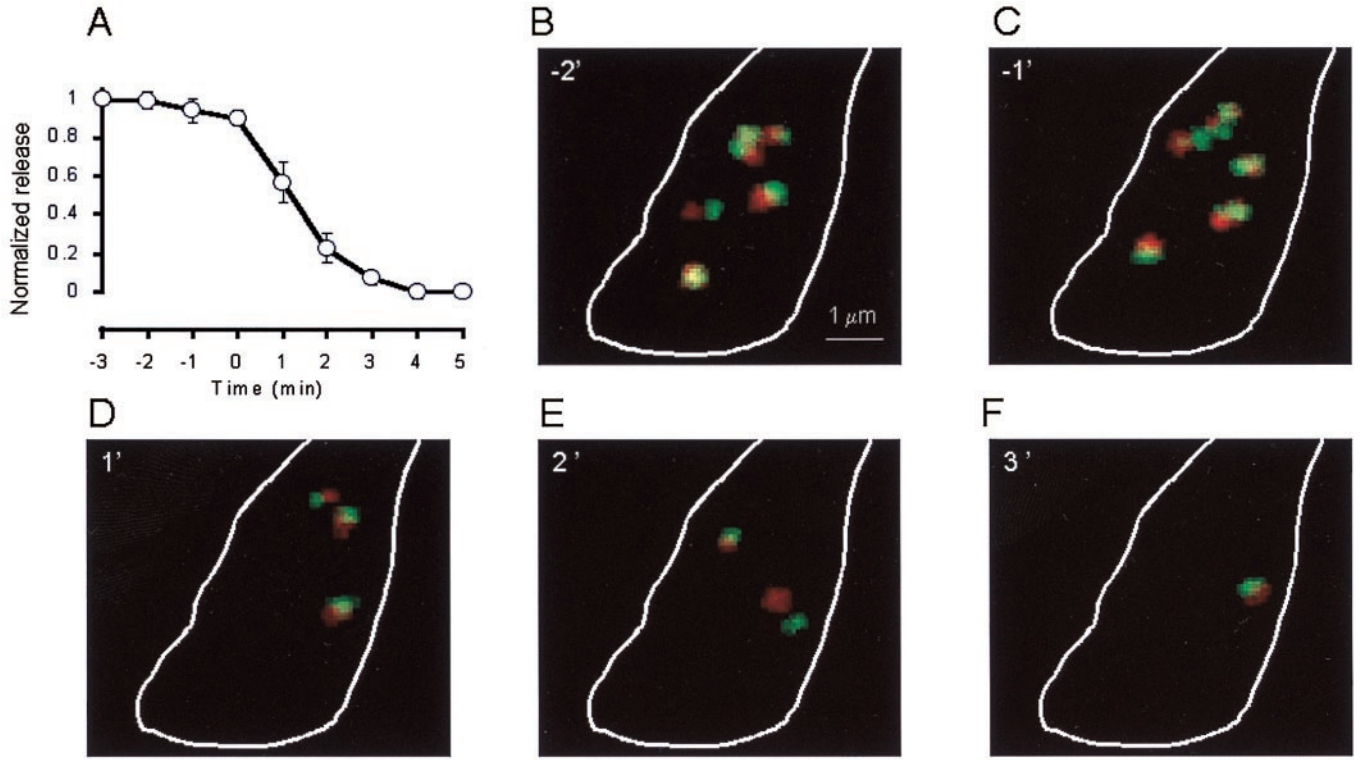

Fig. 5. Mobile vesicles release their contents. (*A*) Normalized time course of peptide release from growth cones with mostly mobile vesicles labeled with the inducible construct. Data derived from epifluorescence measurements from four growth cones. Note that residual fluorescence present after depolarization because of cell autofluorescence, light scattering, and unreleased peptide is not shown in this graph. Sustained depolarization began at 0 min. (*B–F*) Color-coded feature-extracted images of vesicles in a stimulated growth cone. Two images were acquired 5 s apart and then color coded as described in the text. Mobile vesicles appear red or green and stationary vesicles are yellow. The yellow vesicle in *B* subsequently moved, indicating that it was a mobile vesicle that had paused randomly. Note that sustained depolarization causes red and green vesicle images to disappear, indicating that mobile vesicles undergo exocytosis. Similar results were obtained in three other experiments.

disappeared. Importantly, this release occurred with kinetics similar to those seen in our previous studies (4, 19). We also directly tested whether exocytosis and/or immobilization occurred. In these experiments, sets of images were collected before and after depolarization. In each case, the first image of a pair was presented on a green color scale whereas the second image was presented on a red color scale. Therefore, stationary vesicles are represented by both colors and appear yellow. In contrast, vesicles that took large steps produced red and green images. The representative example in Fig. 5 *B–F* shows that stimulation was accompanied by the disappearance of red and green vesicle images. No sustained conversion of red or green vesicles to yellow vesicles was evident in any of the four growth cones examined. The loss of mobile vesicles was not due to movement out of the epifluorescence plane of focus because variations in the plane of focus did not reveal a significant number of "hidden" vesicles, and the integrated epifluorescence signal dropped only upon stimulation. Interestingly, no dramatic change in the pattern of vesicle motion was seen upon depolarization. Thus, stimulated release is supported by capture and exocytosis of rapidly moving vesicles without any qualitative changes in the mechanism of vesicle movement.

Discussion

Technical Advances. In this report a number of novel approaches were employed to study the behavior of single secretory vesicles in growth cones. First, we used the Emerald variant of GFP to produce a stronger fluorescence signal from labeled secretory vesicles. Second, a stable cell line that expresses these labeled vesicles was generated. This system should facilitate many studies of secretion and vesicle dynamics. Third, we employed an inducible expression system to limit the number of labeled vesicles. This approach could be useful to investigators who are concerned with overexpression of GFP-tagged proteins in live cells. Finally, we showed that TIRFM could be used to study vesicles in growth cones. This technique may prove advantageous for studying the cortical cytoskeleton as well as secretion by these specialized structures. Thus, the technical developments presented here may be generally applicable to studies of secretion and other cellular functions.

Vesicle Dynamics in Growth Cones and Bovine Chromaffin Cells. We found that peptidergic vesicle motion is random in growth cones. In chromaffin cells, movement of membrane-proximal "docked" vesicles (6–9) appears to be similar to the slow, immobile vesicles in growth cones. Yet, this similarity may be misleading because vesicles that are docked to the plasma membrane and reserve vesicles that are immobilized in the cytoplasm (4) may have similar trajectories. To date, the movement of immobile cytoplasmic secretory vesicles has not been studied in chromaffin cells, perhaps because acridine orange labeling is not specific and because identifying such reserve vesicles is not simple in TIRFM experiments.

Our data also indicate that mobile cytoplasmic vesicle movement differs between growth cones and endocrine chromaffin cells: undocked cytoplasmic vesicles in chromaffin cells appear to move very rapidly in a directed fashion whereas they move more slowly and randomly in growth cones. The diffusion coefficients for rapid secretory vesicles in growth cones are a thousandfold smaller than expected for diffusion in water, but

are similar to those found for inert, similar-sized beads in cytoplasm (K. Luby-Phelps, personal communication). Thus, it is possible that the fast vesicles we detected are moving by Brownian motion and that their speed is limited by the meshwork of cytoskeleton and the viscosity of the cytoplasm (20). If this is the case, it would suggest that mechanisms for directing movement may be reserved for supporting fast release from small, synaptic vesicles at neuronal sites of release. We also found that the slower, ''immobile'' vesicles appeared to move by diffusion. This implies that these vesicles may be repetitively trapped or tethered to the cytoskeleton as they wander through the cytoplasm. Alternatively, they may be associated with a larger, very slowly diffusing complex that resides in the cytoplasm or is associated with the plasma membrane (e.g., a docking complex). Finally, it is striking that rapidly moving vesicles are very rare in chromaffin cells, refill the docked pool very slowly, and may not be releasable for long periods after arriving to the membrane (6). Thus, rapidly moving vesicles do not appear to have a significant role in supporting the first minutes of hormone release in bovine chromaffin cells. In contrast, mobile vesicles are abundant in growth cones and participate in neuropeptide secretion (see below).

Rapidly Diffusing Cytoplasmic Secretory Vesicles Support Neuropeptide Release. This study was motivated by the fact that the cellular basis of the releasable neuropeptide pool has remained unknown despite decades of study. Previous data were consistent with a conventional model that neuropeptide release is supported solely by docked vesicles and that this spatially delimited depletion is obscured by redistribution of unprimed cytoplasmic vesicles. However, the high-resolution measurements presented here directly show that the releasable pool is markedly different in neuronal growth cones than in bovine chromaffin cells, where a stable population of docked or membrane proximal vesicles accounts for the first 2 min of stimulated release. Although it is possible that there is some participation of previously docked vesicles in growth cones, our data directly demonstrate an efficient capture of rapidly diffusing cytoplasmic secretory vesicles to support the first minutes of neuropeptide release.

It is notable that the distance to the plasma membrane is typically small for vesicles in growth cones and nerve terminals. Therefore, diffusion is a viable mechanism for vesicle translocation at sites of neuropeptide secretion. Interestingly, the findings that vesicles move according to the diffusion equation and that rapidly diffusing vesicles efficiently release their contents establish a basis for quantitative modeling of secretion kinetics. If one assumes that from the view of a cytoplasmic vesicle the growth cone approximates two parallel, adsorbing planes of plasma membrane and that rapidly diffusing vesicles are randomly distributed within the growth cone (see ref. 4), then the average time for vesicles to reach the membrane can be calculated with knowledge of the distance between the top and bottom of the growth cone and the diffusion coefficient of secretory vesicles (21). Based on our findings, this model yields a value greater than a minute. Thus, given our finding that cytoplasmic vesicles release their contents, secretory vesicle diffusion must contribute to the slow rate of sustained neuropeptide release. This raises the possibility that speeding up the biochemical steps involved in docking and exocytosis might have little impact on the amount or kinetics of neuropeptide secretion triggered by prolonged stimuli. Most importantly, the slow kinetics and limited extent of release with a paucity of docked vesicles that characterizes neuropeptide secretion (2, 3, 22, 23) are consistent with the efficient utilization of a limited pool of randomly moving cytoplasmic vesicles.

We thank Drs. R. Grishanin and T. F. J. Martin (University of Wisconsin) for assistance in generating a stable cell line, Drs. Martin and C. Artalejo (Wayne State University) for samples of PC12 cells, and Ms. Danqing Li for excellent technical help. This work was supported by Grant NS32385 from the National Institutes of Health and a pilot project grant from the Cystic Fibrosis Foundation (to E.S.L.). E.S.L. is an Established Investigator of the American Heart Association.

1. Bean, A. J., Zhang, X. & Hokfelt, T. (1994) *FASEB J.* **8,** 630–638.
2. Thorn, N. A. (1966) *Acta Endocrinol.* **53,** 644–654.
3. Sachs, H., Share, L., Osinchak, J. & Carpi, A. (1967) *Endocrinology* **81,** 755–770.
4. Burke, N. V., Han, W., Li, D., Takimoto, K., Watkins, S. C. & Levitan, E. S. (1997) *Neuron* **19,** 1095–1102.
5. Parsons, T. D., Coorsen, J. R., Horstmann, H. & Almers, W. (1995) *Neuron* **10,** 21–30.
6. Steyer, J. A., Horstmann, H. & Almers, W. (1997) *Nature (London)* **388,** 474–478.
7. Oheim, M., Loerke, D., Stuhmer, W. & Chow, R. H. (1998) *Eur. Biophys. J.* **27,** 83–98.
8. Steyer, J. A. & Almers, W. (1999) *Biophys. J.* **76,** 2262–2271.
9. Oheim, M., Loerke, D., Stuhmer, W. & Chow, R. H. (1999) *Eur. Biophys. J.* **28,** 91–101.
10. Axelrod, D. (1989) *Methods Cell Biol.* **30,** 245–270.
11. No, D., Yao, T. P. & Evans, R. M. (1996) *Proc. Natl. Acad. Sci. USA* **93,** 3346–3351.
12. Tsien, R. Y. (1998) *Annu. Rev. Biochem.* **67,** 509–544.
13. Coorssen, J. R., Blank, P. S., Tahara, M. & Zimmerberg, J. (1998) *J. Cell Biol.* **143,** 1845–1857.
14. Seidman, C. E., Graham, A. D., Haber, E., Homcy, J. A., Smith, J. A. & Seidman, J. G. (1984) *Science* **225,** 324–326.
15. Qian, H., Sheetz, M. P. & Elson, E. L. (1991) *Biophys. J.* **60,** 910–921.
16. Crank, J. (1975) *The Mathematics of Diffusion* (Oxford Univ. Press, New York), 2nd Ed.
17. Gundersen, R. W. (1988) *J. Neurosci. Res.* **21,** 298–306.
18. Levitan, E. S. (1998) *Methods* **16,** 182–187.
19. Han, W., Li, D., Stout, A. K., Takimoto, K. & Levitan, E. S. (1999) *J. Neurosci.* **19,** 900–905.
20. Luby-Phelps, K., Taylor, D. L. & Lanni, F. (1986) *J. Cell Biol.* **102,** 2015–2022.
21. Berg, H. C. (1993) *Random Walks in Biology* (Princeton Univ. Press, Princeton, NJ), revised ed.
22. Normann, T. C. (1976) *Int. Rev. Cytol.* **46,** 1–77.
23. Jan, Y. N., Jan, L. Y. & Kuffler, S. W. (1979) *Proc. Natl. Acad. Sci. USA* **76,** 1501–1505.